Measurement of the Correlation between Electron Spin and Photon Linear Polarization in Atomic-Field Bremsstrahlung

S. Tashenov,[1,2,3] T. Bäck,[1] R. Barday,[4] B. Cederwall,[1] J. Enders,[4] A. Khaplanov,[1] Yu. Poltoratska,[4] K.-U. Schässburger,[1] and A. Surzhykov[3,5]

[1]*Royal Institute of Technology, SE-10691 Stockholm, Sweden*
[2]*Stockholm University, SE-10691 Stockholm, Sweden*
[3]*Physikalisches Institut der Universität Heidelberg, 69120 Heidelberg, Germany*
[4]*Institut für Kernphysik, Technische Universität Darmstadt, 64289 Darmstadt, Germany*
[5]*GSI Helmholtzzentrum für Schwerionenforschung GmbH, 64291 Darmstadt, Germany*

(Received 18 November 2010; published 19 October 2011)

Atomic-field bremsstrahlung has been studied with a longitudinally polarized electron beam. The correlation between the initial orientation of the electron spin and the angle of photon polarization has been measured at the photon high energy tip region. In the time reversal this corresponds to a so-far unobserved phenomenon of production of longitudinally polarized electrons by photoionization of unpolarized atoms with linearly polarized photons. The results confirm the fully relativistic calculations for radiative recombination and suggest a new method for electron beam polarimetry.

DOI: 10.1103/PhysRevLett.107.173201 PACS numbers: 34.80.Nz, 32.80.Fb, 41.60.−m

Atomic-field bremsstrahlung is a dominant radiative process in relativistic electron-atom collisions. Its studies are fundamental for the understanding of electromagnetic interactions in the realm of strong fields provided by heavy nuclei. In this hard x-ray regime the coupling of an electromagnetic field with matter differs significantly from the low energy regime. In particular, relativistic and higher order multipole effects have been observed in studies of linear photon polarization with unpolarized electron beams [1,2]. These effects are especially pronounced at the high energy tip region of the photon spectrum [3]. At these energies bremsstrahlung probes the dynamics of the electron at close distances to the nucleus where the electric and the induced magnetic fields are the strongest and the influence of the electron spin is the largest. Strong effects of the spin-orbital interaction were observed via left-right asymmetry of bremsstrahlung from transversally spin-oriented electrons [4]. This high energy tip region might also be considered as the Rydberg series limit of radiative recombination (RR) [5,6] and therefore it also describes the spin dynamics of the fundamental process of photoionization in time reversal [7]. Relativistic theories predict that more differential studies of linear polarization of photons emitted by polarized electrons, with a particular emphasis on the angle of polarization, should reveal significantly finer details of the spin dynamics of electrons in strong fields [3,8]. Such polarization studies, however, were stalled for two decades due to the complexity of the angle-resolved hard x-ray polarimetry, and only recently became possible.

Apart from their fundamental interest, bremsstrahlung linear polarization and electron beam spin properties come into play in many areas of physics. Bremsstrahlung is commonly used as a source of radiation for a variety of applications. Linear polarization from off-axis bremsstrahlung is used to determine multipolarities of nuclear transitions in nuclear resonance fluorescence experiments [9,10]. Energetic electrons in cosmic sources of synchrotron radiation (e.g., in the Crab Nebula) should also emit bremsstrahlung. Such electrons may acquire polarization due to the spin dependence of synchrotron radiation [11], as observed at electron storage rings [12]. Longitudinally polarized electrons and positrons are also emitted by beta-decaying nuclei created in supernova explosions. Polarization correlations will strongly influence linear polarization of bremsstrahlung from such electrons and positrons. Future polarization-sensitive big satellite-based x-ray and gamma-ray telescopes [13–15] will be sensitive to such effects.

In this Letter we report the first measurement of a correlation between longitudinal polarization of an electron beam and the angle of linear polarization of bremsstrahlung photons. With Compton and Rayleigh scattering polarimetry techniques we achieved sensitivity of 7 mrad to the angle of linear polarization of hard x rays, which is by at least 1 order of magnitude higher than in any previous measurement in this energy range. This allowed us to observe the rotation of photon polarization out of the bremsstrahlung reaction plane which exposes the spin-induced dynamics of the electron moving in the strong field of a heavy nucleus. The rotation angle ψ can be described in terms of the Stokes parameters P_1 and P_2 as $\tan 2\psi = \frac{P_2}{P_1}$; see, e.g., Refs. [16,17]. The observed effect thus corresponds to the nonzero second Stokes parameter P_2. The novel technique of Rayleigh scattering photon polarimetry [18] was used for the first time. It can also be considered that we observed a time reversal of a hitherto experimentally unknown aspect of photoionization—

 © 2011 American Physical Society

production of longitudinally polarized electrons with unpolarized atoms and linearly polarized photons [19]. These phenomena allow for much-demanded novel techniques for polarimetry of electron and heavy-ion beams.

The measurement was performed at a test stand of a newly constructed source of longitudinally polarized electrons at Technische Universität Darmstadt, Germany [20]. The electrons were accelerated electrostatically to 100 keV. The degree of polarization of the electron beam $P_e = 75 \pm 4\%$ was determined using Mott scattering [21] together with a Wien filter [22].

The bremsstrahlung photons were produced in the gold foil target. With its thickness of 200 nm, effects of multiple electron scattering were pronounced. Since the individual photons are linearly polarized relative to the directions of the individual electrons, the total degree of photon polarization was reduced. Nevertheless, due to the axial symmetry of the electron beam and the target, the mean electron direction was preserved. Therefore the angle of photon polarization was not affected by multiple scatterings.

Compton and Rayleigh scattering techniques were used to measure linear polarization of the emitted hard x rays. A high purity planar germanium detector was applied for this purpose. The active detector area of 5×5 cm is segmented into a 5×5 matrix of square pixels. Each pixel is equipped with an individual charge sensitive preamplifier and a sampling analog-to-digital converter, yielding an energy resolution of 2.7 keV at 60 keV. The detector thickness is 2 cm.

The detector was placed at a distance of 15 cm from the gold target, see Fig. 1, behind a 3 mm thick vacuum chamber quartz window (not displayed). The window transmission at 90–100 keV was >86%. GEANT4 Monte Carlo simulations [23] have shown that the influence of scatterings of photons in the window on their linear polarization was negligible. Lead walls with a thickness of 1 cm shielded the detector from unwanted x rays. The bremsstrahlung was collimated by a 1 cm round opening in the shield, which selected photons emitted at $90° \pm 3°$ with respect to the electron beam direction. The variation of photon polarization within this angle interval is negligible. The detector was placed perpendicular to the photon beam. Its axis was aligned with the collimated photon beam axis. A photon scattering target has been placed behind the collimator at the distance of 2.7 cm from the detector crystal. With this arrangement the outer detector segments, used in the analysis, could observe only the scattered photons.

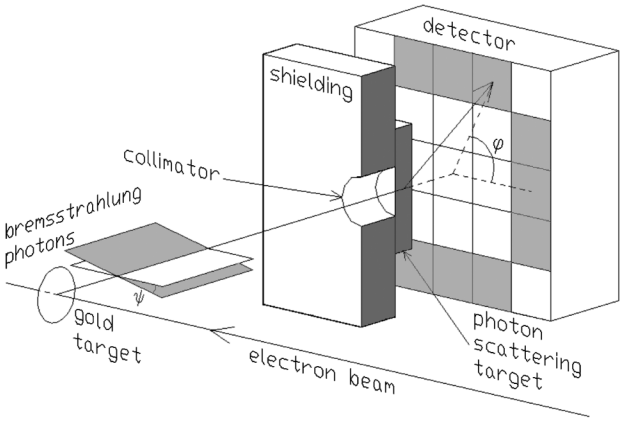

FIG. 1. Scheme of the experimental setup (the shielding and the scattering target are shown in section). The reaction plane (white) is defined by the incoming electron and the emitted photon directions. The photon linear polarization plane (gray) is tilted by an angle ψ with respect to the reaction plane. The azimuthal photon scattering angle is denoted by φ. Detector segments used in analysis are indicated in gray.

The photon scattering target was optimized for the polarization measurement at the bremsstrahlung high energy tip region. For this the low energy photons were absorbed. An iron scatterer of 5 mm thickness has been selected for its high photoabsorption below ≈ 75 keV and high probability of photon scattering at higher energies. The geometry with a separate passive scatterer provided advantages as compared to an active scatterer technique used in earlier measurements [24]: the count rate was not limited by the dead time in the active scatterer and the photons had only minimal attenuation between the scatterer and the absorber.

A typical measured spectrum at the tip region is shown in Fig. 2. The contributions of Compton and Rayleigh scatterings have been determined via Monte Carlo simulations. Rayleigh scattering accounts for 15% of events in the spectral interval "*a*" and for 72% in the interval "*b*."

The radiation background, superimposed with the true bremsstrahlung spectrum, originated from bremsstrahlung of electrons which elastically scattered in the gold target and hit the chamber quartz window. Except for this window the chamber was covered by a lead x-ray absorber. To calculate the emitted background radiation, the following model was adopted. Electrons lose energy as they penetrate through quartz. Their energy was calculated as a function

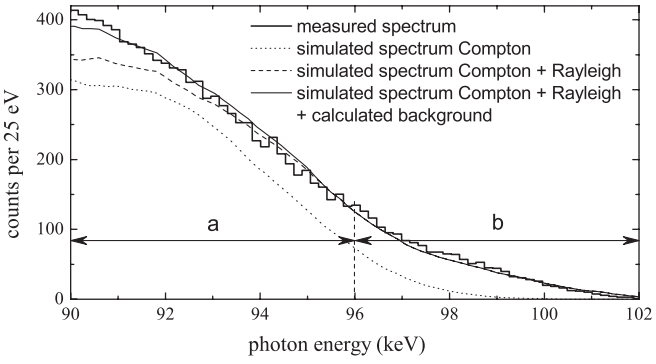

FIG. 2. Measured and simulated spectra. Contributions of Compton and Rayleigh scatterings as well as background are shown separately. Intervals *a* and *b* were analyzed separately.

of the penetration depth using the continuous slowing down approximation [25]. For each electron energy the penetration depth provided an effective thickness of the quartz layer as a bremsstrahlung target. For each layer and an appropriate electron energy, the bremsstrahlung spectrum was calculated and summed up. With this procedure the background contribution in the energy interval a was determined to be 7%, and negligible in the interval b; see Fig. 2.

The polarization-sensitive scattered photon angular distributions $I(\varphi)$ from the spectral intervals a and b have been analyzed individually. Within these intervals the energy dependence of $I(\varphi)$ could be neglected. In order to minimize systematic effects caused by a possible slight misalignment of the collimator with respect to the detector's axis, an intensity normalization $J(\varphi) = \frac{I(\varphi+90°)+I(\varphi+270°)}{I(\varphi)+I(\varphi+180°)}$ has been performed, utilizing the detector's fourfold rotational symmetry; see Fig. 3(a). As a result of the Compton and Rayleigh scattering, the normalized scattered photon azimuthal angular distribution is $F(\varphi, M) = \frac{1-M\cos^2(\varphi+90°)}{1-M\cos^2(\varphi)}$, where φ is an azimuthal angle with respect to the polarization plane and M is a modulation which depends on the degree of polarization and the angle between the initial and scattered photon directions [18,24]. The azimuthal modulation of photon scattering in the interval a was $M = 25\%$.

For each scatterer two measurements with opposite orientations of the electron spins were taken, while keeping all other experimental conditions fixed. As a result of the mirror reflection symmetry with respect to the reaction plane, the modulations of $J_{\mathrm{col}}(\varphi)$ and $J_{\mathrm{anticol}}(\varphi)$ must be equal and the corresponding photon polarization planes must be tilted to opposite directions by equal angles ψ, thus producing a 2ψ phase shift between these distributions.

To cancel effects of geometrical differences of individual segments, the scattering angular distributions were normalized $\frac{J_{\mathrm{col}}(\varphi)}{J_{\mathrm{anticol}}(\varphi)}$; see Fig. 3(b). The modulation of the normalized distribution is roughly proportional to ψ; i.e., it must be zero when $\psi = 0$. In the interval a this modulation is only 3.5%. Because of geometrical constrains the detector was tilted by an angle $\varphi_0 = 2.81°$ relative to the reaction plane, which shifts the normalized distribution but does not change its modulation. To extract ψ, the normalized distribution $\frac{J_{\mathrm{col}}(\varphi)}{J_{\mathrm{anticol}}(\varphi)}$ has been fitted with a function $\frac{F(\varphi+\varphi_0+\psi,M)}{F(\varphi+\varphi_0-\psi,M)}$, treating ψ as a single free parameter. The extracted value of the tilt angle ψ has then been normalized on the degree of electron polarization P_e. The results are shown in Table I. Average initial photon energies were obtained via Monte Carlo simulations.

TABLE I. Measured and calculated tilt angles of bremsstrahlung linear polarization with respect to the reaction plane.

Spectral interval	Analysis method	Incoming photon energy (keV)	Polarization angle (deg)
a	Compton	95.5 ± 2.4	2.1 ± 0.4
b	Rayleigh	97.9 ± 1.5	2.1 ± 0.7
...	Theory	100	2.17

The rotation of linear polarization can be qualitatively explained based on classical electrodynamics. The axial symmetry of the collision is broken due to the high azimuthal correlation between the electron scattering and the photon emission directions. We define the **yz** plane by the initial electron and the emitted photon momenta. The magnetic field **H** produced in the electron rest frame by the target nucleus causes the electron spin precession; see Fig. 4(a). The nuclear charge Z is partially screened; however, the screening effects are negligible at 100 keV [26]. The electrons with initial momenta parallel to **z** and above and below the **yz** plane will be deflected along **x** to opposite directions; see Figs. 4(b) and 4(c). However, due to the finite spin component $\mathbf{s_y}$ and the spin-orbit coupling in Mott scattering [22], the magnitudes of these deflections will be different; see Fig. 4(c). The preferred direction of electron deflection along **x** prior to the photon emission causes the tilt of the instantaneous scattering plane which is

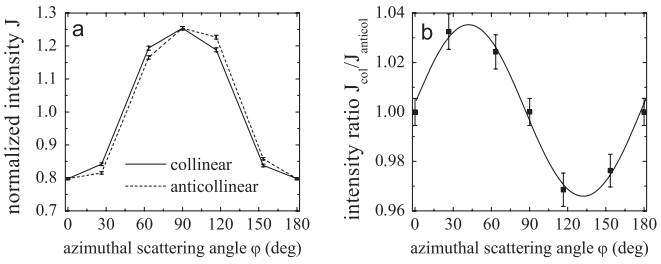

FIG. 3. (a) Normalized scattering intensity angular distribution for scattering of bremsstrahlung from the spectral interval a from the collinearly $[J_{\mathrm{col}}(\varphi)]$ and anticollinearly $[J_{\mathrm{anticol}}(\varphi)]$ polarized electron beams. (b) Intensity ratio $J_{\mathrm{col}}(\varphi)/J_{\mathrm{anticol}}(\varphi)$.

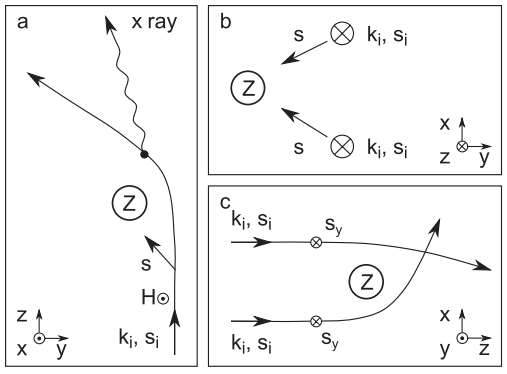

FIG. 4. Classical description of the origin of the tilted scattering plane prior to the photon emission. Projections along **x**, **y**, and **z** are shown in (a), (c), and (b), respectively. The initial electron momentum and spin are denoted by $\mathbf{k_i}$, $\mathbf{s_i}$.

the origin of the tilted photon polarization plane and the nonzero second Stokes parameter P_2.

In addition to the experimental results, Table I also displays the theoretical prediction for the tilt angle ψ obtained for the photon high energy limit. To evaluate ψ for this particular energy we have extrapolated the results of the RR polarization calculations towards the continuum threshold. Such a computational approach has been justified for the tip region in a number of works (see, for example, [6] and references therein). In the present contribution, the polarization of the RR photons emitted due to the recombination of longitudinally polarized electrons into bound high-n states has been calculated within the fully relativistic theory. Since this theory has been applied very frequently in studying various RR properties we will not discuss it here and instead refer the reader to Refs. [16,17,27,28]. As seen from Table I, the theoretical value of the tilt angle ψ, obtained from the extrapolation of the rigorous RR calculations to the tip region, is in good agreement with the experimental findings. The predicted energy dependence of ψ below the tip region was small [26] in comparison with the experimental error bars.

Photoionization, a time reversal of RR, exhibits similar polarization correlations [19]. It was known (e.g., in the Fano effect [29]) that as a consequence of the angular momentum conservation the photon helicity (spin orientation) can be transferred to longitudinal polarization of the photoelectrons. However, the observed polarization correlation at the high energy tip of bremsstrahlung demonstrates in time reversal the production of longitudinally polarized electrons by linearly polarized photons, i.e., by photons with no defined spin orientation.

The experiment also confirms the theory of RR into polarized H-like ions and leads to a unique method of heavy-ion beam polarimetry [17]. Such a method is highly demanded for parity nonconservation experiments as tests of the standard model of particle physics [30,31]. In a similar way, bremsstrahlung can be applied for polarimetry of electron beams. At relativistic energies the tilt angle ψ will vary by tens of degrees as a function of electron polarization [26,32,33], which should facilitate electron polarimetry.

This work was supported by the Swedish Research Council, Contract No. 2007-4067, and the Göran Gustafsson Foundation. The Darmstadt group acknowledges financial support by DFG through SFB 634 and by the state of Hesse through the Helmholtz International Center for FAIR within the LOEWE program. S. T. acknowledges support by the German Research Foundation (DFG) within the Emmy Noether program under Contract No. TA 740 1-1. A. S. acknowledges support by the Helmholtz association under the project VH-NG-421.

[1] R. W. Kuckuck and P. Ebert, Phys. Rev. A **7**, 456 (1973).
[2] W. Lichtenberg *et al.*, Phys. Rev. A **11**, 480 (1975).
[3] E. Haug, Phys. Rev. **188**, 63 (1969).
[4] E. Mergl *et al.*, Phys. Rev. Lett. **69**, 901 (1992).
[5] M. Nofal *et al.*, Phys. Rev. Lett. **99**, 163201 (2007).
[6] I. J. Feng *et al.*, Phys. Rev. A **28**, 609 (1983).
[7] K. W. McVoy and U. Fano, Phys. Rev. **116**, 1168 (1959).
[8] H. K. Tseng and R. H. Pratt, Phys. Rev. A **7**, 1502 (1973).
[9] U. E. P. Berg and U. Kneissl, Annu. Rev. Nucl. Part. Sci. **37**, 33 (1987).
[10] K. Govaert *et al.*, Nucl. Instrum. Methods Phys. Res., Sect. A **337**, 265 (1994).
[11] A. A. Sokolov and I. M. Ternov, Sov. Phys. Dokl. **8**, 1203 (1964).
[12] B. W. Montague, Phys. Rep. **113**, 1 (1984).
[13] E. Costa *et al.*, Proc. SPIE Int. Soc. Opt. Eng. **7011**, 70110F (2008).
[14] S. E. Boggs *et al.*, New Astron. Rev. **48**, 251 (2004).
[15] M. Jackson *et al.*, IEEE Nucl. Sci. Symp. Conf. Rec. **8**, 449 (2009).
[16] A. Surzhykov *et al.*, Phys. Rev. A **68**, 022710 (2003).
[17] A. Surzhykov *et al.*, Phys. Rev. Lett. **94**, 203202 (2005).
[18] S. Tashenov *et al.*, Nucl. Instrum. Methods Phys. Res., Sect. A **600**, 599 (2009).
[19] R. H. Pratt *et al.*, Phys. Rev. **134**, A916 (1964).
[20] Y. Poltoratska *et al.*, AIP Conf. Proc. **1149**, 983 (2009).
[21] T. J. Gay and F. B. Dunning, Rev. Sci. Instrum. **63**, 1635 (1992).
[22] M. Salomaa and H. A. Enge, Nucl. Instrum. Methods **145**, 279 (1977).
[23] S. Agostinelli *et al.*, Nucl. Instrum. Methods Phys. Res., Sect. A **506**, 250 (2003).
[24] S. Tashenov *et al.*, Phys. Rev. Lett. **97**, 223202 (2006).
[25] ICRU Report No. 37, 1984 (unpublished).
[26] V. A. Yerokhin and A. Surzhykov, Phys. Rev. A **82**, 062702 (2010).
[27] J. Eichler and Th. Stöhlker, Phys. Rep. **439**, 1 (2007).
[28] S. Fritzsche, A. Surzhykov, and Th. Stöhlker, Phys. Rev. A **72**, 012704 (2005).
[29] U. Fano, Phys. Rev. **178**, 131 (1969).
[30] L. N. Labzowsky *et al.*, Phys. Rev. A **63**, 054105 (2001).
[31] A. V. Nefiodov *et al.*, Phys. Lett. B **534**, 52 (2002).
[32] D. H. Jakubassa-Amundsen, Phys. Rev. A **82**, 042714 (2010).
[33] D. H. Jakubassa-Amundsen and A. Surzhykov, Eur. Phys. J. D **62**, 177 (2011).